Talanta 268 (2024) 125360

Contents lists available at ScienceDirect

Talanta

journal homepage: www.elsevier.com/locate/talanta

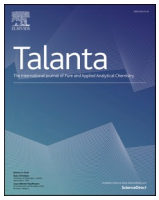

sp-ICP-MS and HR–CS–GFAAS as useful available techniques for the size characterization and speciation of ionic and nanoparticular zinc in cosmetic and pharmaceutical samples

J.C. García-Mesa [1], I. Morales-Benítez [1], P. Montoro-Leal [1], M.M. López Guerrero [*], E.I. Vereda Alonso [**]

Department of Analytical Chemistry, Faculty of Sciences, University of Malaga, 29071, Málaga, Spain

ARTICLE INFO

Handling Editor: J. Wang

Keywords:
ZnO NPs
Cosmetics
sp-ICP-MS
HR–CS–GFAAS
Speciation

ABSTRACT

The use of zinc oxide nanoparticles (ZnO NPs) in cosmetic and pharmaceutical industry has been increased in recent years due to their good properties as solar radiation filters and antibacterial agent. According to the literature, the potential toxicity of these NPs could be size-dependent and the amount of solubilized metal. This work investigates new reliable and straightforward methodologies that enables the determination of ZnO NPs, discriminating them from ionic zinc in cosmetic samples. Two different techniques of analysis have been applied in this study: high-resolution continuum source graphite furnace atomic absorption spectrometry (HR–CS–GFAAS), and "single particle" inductively coupled plasma mass spectrometry (sp-ICP-MS). Triton X-100 has been used as a surfactant for the formation of homogeneous and stable slurries which allowed the determination of the concentration and sizes of ZnO NPs and Zn^{2+} in baby creams, eyeshadows, and lotions. A central composite design (CCD) was performed for the two techniques to optimize the concentration of Triton X-100 and sonication time. For validation purpose, the results of Zn^{2+} and ZnO NPs contents achieved by HR–CS–GFAAS were compared with the total Zn content obtained by acid digestion of the samples. A size comparison of the ZnO NPs was also carried out with the data obtained through the two methodologies and validated with transmission electron microscopy (TEM). In the case of TEM analysis, two different media were tried to study possible agglomerates and interactions between the particles and the matrix.

1. Introduction

Even before their unique extraordinary properties were known, nanomaterials (NMs) and nanoparticles (NPs) had come into use. Nowadays, the application of nanotechnology has generated important benefits, widely recognized. Materials based on nanotechnology or containing engineered NPs represent a true scientific revolution. A multitude of products that surround our lives are manufactured and/or containing NPs, in diverse fields such as cosmetics, food, textiles, electronics, construction and medicine [1,2]. During the use of these products or after their disposal, different types of NPs are released into the environment. Consequently, the exposure to them is increasing, and their effects on the environment or human health are currently being questioned [3]. Due to their tiny size (1–100 nm), NPs can be introduced in the human body by inhalation, ingestion, or skin penetration. The same exceptional physical and chemical properties of NMs and NPs, make them also potentially toxic: high surface reactivity, high stability, and the facility to penetrate the bloodstream to reach different organs of the body [4]. A variety of NPs, such as TiO_2, ZnO, silver, silica and iron oxides are really extended, being the consumers directly or indirectly exposed to this kind of materials [5].

TiO_2 and ZnO NPs are the two key ingredients used in sunscreens because they can reflect and scatter UVA and UVB radiations while preventing skin irritation and disruption of the endocrine system typically induced by organic UV filters [6]. As ZnO NPs do not scatter visible light, they appear to be transparent, in contrast with other products that may appear to be an opaque white color [7]. Furthermore, ZnO NPs are compatible with skin, protecting it from irritants agents due to

* Corresponding author.
** Corresponding author.
E-mail addresses: mmlopez@uma.es (M.M. López Guerrero), eivereda@uma.es (E.I. Vereda Alonso).
[1] Equally contribution.

https://doi.org/10.1016/j.talanta.2023.125360
Received 1 August 2023; Received in revised form 16 October 2023; Accepted 26 October 2023
Available online 29 October 2023

antimicrobial, antioxidant, and anti-inflammatory properties [8]. ZnO NPs are commonly used for treating different skin conditions. In addition, they have emerged as a suitable tool in drug delivery. For all these reasons, ZnO NPs are one of the NPs more employed in cosmetic and medicine [9]. However, like other NPs, the enhanced antimicrobial properties of these NPs, make them one of the most harmful NPs in aquatic exposures, though this toxicity can be attributed to the solubilized metal from NPs in solution [10]. Results of several studies revealed that ZnO NPs were soluble partially, up to 20 μg mL^{-1} after a day and could induce strong cytotoxicity as compared with other insoluble NPs [1,11]. After all these considerations, reliable analysis methods are needed, capable of characterizing and determining ZnO NPs and discriminating them from ionic zinc in different types of samples, pharmaceutical, cosmetic, etc, with the additional challenge of its determination in complex matrices. Samples with complex matrices could require pre-treatments that enable quantitative NPs separation while still ensuring their integrity (specially their size). A detailed description of the advantages and limitations of sample preparation procedures for metallic and metal oxide NPs characterization in consumer products can be found in the review article by de la Calle et al. [12].

Currently, the full characterization of NPs in complex matrices without misleading dilution or modification is a challenging goal for the analytical chemistry. Microscopic techniques (Transmission Electron Microscopy, TEM and Scanning Electron Microscopy, SEM), and light scattering techniques (Dynamic Light Scattering, DLS and Multi-angle Laser Light Scattering, MALLS) are of great value to determine size parameters of NPs. However, these techniques are not able to quantify the concentration of the different metal species in the samples [13]. Among spectroscopic and spectrometric techniques capable of providing information about chemical composition such as Inductively Coupled Plasma Mass Spectrometry (ICP-MS), Inductively Coupled Plasma Optical Emission Spectrometry (ICP-OES), and Atomic Absorption Spectrometry (AAS), Single Particle Detection mode ICP-MS (sp-ICP-MS), the last one has increasingly gained importance. The advantages of using sp-ICP-MS are high throughput and the capacity to obtain information on particle size and particle number concentration, as well as being widely available in many laboratories [14]. In sp-ICP-MS, metal or metal oxide-based NPs in a sample are introduced as a diluted suspension into the plasma torch producing a plume of metal ions. This plume is detected as a signal pulse in the MS, allowing the determination of NPs concentration in the sample by monitoring the atomic mass of the metal. If the mass, composition, and density of the NP are known, and the NP shape is assumed to be spherical (generally) or other simple shape, the particle size can be estimated. To ensure that each signal pulse is originated from one NP only, adequate time resolution and a low NPs concentration are required. Therefore, samples must be normally diluted enough to prevent the simultaneous detection of two or more NPs [14]. sp-ICP-MS is turning into a powerful technique for the quantification and characterization of metallic NPs. Notwithstanding, this technique has relatively high size detection limits for highly soluble nanoparticles (e.g. ZnO, CuO) or NPs that are measured in the presence of high background concentrations of dissolved metal [15]. Unfortunately, significant dissolution of the ZnO NPs generally increases background levels of dissolved zinc, making very difficult to distinguish between NPs events and the background signal due to dissolved metal. This is the reason why up to date, sp-ICP-MS has been mainly used for the characterization of gold [3,16–18], silver [3,16,19,20], and TiO_2 [3,21–23]; little success has been obtained for highly soluble NPs, such as ZnO NPs [15,24]. In both referenced articles, the use of an ion exchange column was described to eliminate the dissolved metal.

In a recent paper [25], a direct solid sampling method for speciation of Zn^{2+} and ZnO NPs in eyeshadows by High Resolution Continuum Source Graphite Furnace Atomic Absorption Spectrometry (HR–CS–GFAAS) was optimized and validated by us. The direct solid sampling has the advantage of the no-necessity of sample pretreatment neither suspensions preparation. Gagné et al. [26] were the first authors that reported NPs identification using GFAAS, these authors observed an increase in the atomization temperature for Ag NPs. Since then, other authors have employed HR–CS–GFAAS for the determination and characterization of NPs, Feichtmeier and collaborators [27,28] indicated the possibility to differentiate between Ag^{+} and Ag NPs through the evaluation of atomization delays, the same parameter was used by Resano et al. [29]. Vereda Alonso et al. [30] used the upslope of the atomization peak to determine the size of magnetic NPs. Brandt et al. [31] investigated the use of GFAAS to characterize size of Au, Ag, Pd, Pt and Fe NPs. All these works demonstrated the possibility to distinguish the ionic species from NPs forms of metals based on their atomization delay, and the size of the metallic NPs with the atomization velocity (upslope of the atomization peak). However, the distance between atomization peak of ionic metal and the metallic NP is small and the peaks appear overlapped. In our previous study [25], the deconvolution of the atomization peaks was necessary to realize the speciation analysis. Other authors have also performed speciation analysis with the use of the named "simulation-assisted calibration" methods and employing the derivative of atomization peak for gold and silver by GFAAS, avoiding the necessity of the deconvolution of their signals into single components [32,33].

In this work, the optimization of two methodologies to speciate ionic Zn^{2+} and ZnO NPs and to obtain ZnO NPs size information by sp-ICP-MS and by HR–CS–GFAAS has been developed. Both methodologies imply the use of adequate suspensions of the samples in Triton X-100. Both methodologies were successfully compared.

2. Experimental

2.1. Instrumentation

In this work, the results obtained by two analytical techniques were compared. For this purpose, most of the experiments were performed on a high-resolution continuum source graphite furnace atomic absorption spectrometer (HR–CS–GFAAS) and on a quadrupole-based inductively coupled plasma mass spectrometers (ICP-MS).

The HR–CS–GFAAS used was a ContrAA 700 (Analytik Jena AG, Jena, Germany), equipped with an autosampler SSA 600 for solid sampling (Sartorius, Goettingen, Germany). This instrument has a complex optical system which consists in a xenon short arc lamp (GLE, Berlin, Germany) operating in "hot-spot" mode as the radiation source, a high-resolution double echelle monochromator (DEMON) and a linear CCD array detector with 588 pixels. 200 of these pixels are used for background corrections and the monitorization of the analytical signal, while the rest carry out internal functions, such as correcting for fluctuations in the lamp intensity. The solid samples were introduced as suspensions for the experiments in a transversely heated pyrolytic graphite tubes with graphite platforms. Data evaluation was achieved with the software ASPECT CS 2.1.2.0 (Analytik Jena AG, Jena, Germany) and Multipak 9.0 Data Reduction Software (Physical Electronics, Chanhassen, MN, USA). The optimum instrumental operation conditions were summarized in Table 1.

ICP-MS NexION 2000 (PerkinElmer, MA, USA), equipped with the Syngystix Nano Application module software (version 2.2) for sp-ICP-MS analysis. NexION 2000 offers a high sensitivity, so smaller NPs can be analysed. Instrumental details and operating conditions used with this instrument are summarized in Table 2. Daily performance check and nebulizer gas flow rate were adjusted so that Ce^{++} (70)/Ce^{+} (140) and CeO^{+} (156)/Ce^{+} (140) ratios were equal to or less than 0.03 and 0.025, respectively. Additionally, cross calibration of the counting to the analog conversion factor for the detector was daily performed before analyses.

For validation purposes, the cosmetic samples were digested using a microwave oven Multiwave 3000 (Anton Paar, Graz, Austria).

All the samples were characterized by TEM. Moreover, these

Table 1
HR–CS–GFAAS optimized instrumental parameters.

Wavelength			307.590 nm	
Number of detector pixels summed per line			3 (4.20 p.m.)	
Temperature program				
Step	**Temperature (°C)**	**Ramp (°C s^{-1})**	**Hold time (s)**	**Ar gas flow (L min^{-1})**
Drying	80	6	20	2.0
Drying	90	3	40	2.0
Drying	110	5	20	2.0
Pyrolysis	150/300[a]	3/50[a]	6/20[a]	2.0
Gas adaptation	150	0	5	0.0
Atomization	1350	1000/1500[a]	3	0.0
Cleaning	2450	500	4	2.0

[a] Conditions for solid sampling analysis of total zinc.

Table 2
ICP-MS operation conditions and sp-ICP-MS method parameters.

	NexION 2000
RF power (W)	1600
Nebulizer Gas flow (L min^{-1})	0.98
Plasma Gas flow (L min-1) rowhead	15
Auxiliary gas flow (L min^{-1})	1.2
Sample introduction system	Glass cyclonic spray chamber-Meinhard Type C glass nebulizer
Sampler cone	Ni
Skimmer cone	Ni
Analyte	ZnO, Au
Mass (amu)	81, 197
Dwell time (μs)	100
Scan time (s)	300
Detection mode	Dual (counting + analog)
NP parameters for calculations	
Density (g cm^{-3})	5.61 (ZnO), 19.3 (Au)
Sample introduction parameters	
Sample uptake rate (μL min^{-1})	300

NPs dilutions were vortexed in a Lab Dancer S040 (IKA®-Werke GmbH & Co. KG, Germany) immediately before their use.

analyses were carried out in two different conditions: samples suspended in ethanol, and samples suspended in the optimized slurry conditions (Triton X-100). For this, a JEM-1400 TEM instrument (Peabody, MA, USA) was employed for measuring the particle size distribution.

2.2. Reagents, standards, and samples

All experiments were carried out with reagents and standards with analytical quality or superior. Doubly de-ionized water (18 MΩ cm) obtained from a Milli-Q water system (Millipore, Bedford, MA, USA) was used throughout for dilutions. Ionic calibration standards were prepared from 1000 mg L^{-1} stock standard solutions (Merck, Darmstadt, Germany) of Zn and Au. Solid ZnO NPs UV Shielding Powder standards (US Research Nanomaterials Inc., Houston, USA) with different sizes between 18 and 500 nm were used in this work. A certified standard of 100 nm Au NPs (PerkinElmer, MA, USA) was also used. The certified values of size and size distributions for all the NPs standards were verified by performing TEM analysis. Homogeneous and stable NPs suspensions of the standards and samples were achieved using the surfactant Triton X-100 (Merck, Darmstadt, Germany) and sodium dodecyl sulphate (SDS) (Merck, Darmstadt, Germany). Concentrated HNO_3 and H_2O_2 (Merck, Darmstadt, Germany) were also used for samples digestions.

Ten samples of cosmetics and personal care products were studied. Five compact powder eyeshadows of different colors (numbered 1 to 5), three baby skincare creams (named A, B and C), and two selfcare lotions (named 1 and 2) samples of several brands were purchased in cosmetic shops in Malaga, Spain.

2.3. Sample preparation

Considering that commercial cosmetics are not usually homogeneous, and to avoid problems with the analysis reproducibility, the samples were manually homogenized for 5 min. Then, after homogenization, an amount of sample (mg) was dispersed in Triton X-100. For GFAAS analysis, samples were prepared 0.1 % (w/w) in 0.55 % Triton X-100 aqueous solution and the suspension was sonicated for 3 min. In the case of sp-ICP-MS analysis, samples were prepared 1–2 % (w/w) in 1 % Triton X-100 aqueous solution, and the suspension was sonicated for 70 min. The NPs suspensions were shaken in a vortex for a few minutes before dilution, to avoid possible particle agglomeration. The dilution factors needed for all the NPs dispersions to minimize the occurrence of double events during sp-ICP-MS measurements were calculated based on Poisson statistics [34] for a dwell time of 100 μs for Au and ZnO NPs standards. In the case of the samples, different studies were carried out to achieve a suitable dilution and stable suspension. In all cases, possible agglomerates are avoided, and well dispersed samples were obtained (white milky suspensions for creams and lotions, and colored milky suspensions for eyeshadows). The stability of the suspensions was tested with the non-appearance of precipitates, and the reproducibility of the results obtained in replicated measures, all of them made with at least six replicates.

2.4. Description of the performed analysis

In this work, the study of Zn species was achieved using two new innovative analysis strategies which can provide all this information. In Fig. 1, a scheme of the different performed analysis is showed.

2.4.1. Total zinc determination

For the total Zn determination in the cosmetic samples, an acid digestion of the samples was carried out in a microwave oven. The selected conditions for the microwave digestion procedure were similar to the applied in a previous work [25]: an accurately weighed amount of sample (0.1–0.15 g) was introduced into a digest vessel with 1.5 mL 65 % HNO_3 and 0.5 mL of 30 % H_2O_2. These vessels containing the mixture were put into the microwave oven at 900 W for 30 min, reaching a temperature of 200 °C. After cooling, the digested samples were evaporated to dryness to eliminate the excess of acids and diluted with de-ionized water in 25 mL volumetric flasks. Aliquots of 20 μL of the samples were injected into the graphite tube for analysis of total Zn by GFAAS. In order to determine the total Zn, different volumes of 30 mg L^{-1} of ionic Zn standard solution were introduced in the graphite furnace (0, 5, 10, 20, and 30 μL) for the calibration curve.

2.4.2. HR–CS–GFAAS measurement protocol

HR–CS–GFAAS has been used for nanoparticle characterization (size and concentration) [26]. In this work, all the cosmetic and pharmaceutical samples were suspended in Triton X-100 and sonicated previously to their analysis by HR–CS–GFAAS. For this, different aliquots of the slurry samples were deposited in the graphite platform of the solid autosampler. The GFAAS system was operating in solid mode. The measurements of Zn were taken using the conditions summarized in Table 1. A mixture of 15 mg L^{-1} of Zn^{2+} (aqueous standard solution) and 0.1 % (w/w) solid ZnO NPs (UV Shielding Powder standards) was prepared as a stock solution. In order to build the calibration curves for both Zn species, different volumes (2.5, 5, 10, 15 and 20 μL) of this stock solution were directly injected into the solid sampling platform.

The upslope of nanoparticular peak (the second one) was used to obtain the size value. For the calibration, the ZnO NPs UV Shielding Powder standards between 18 and 500 nm were used for calibration.

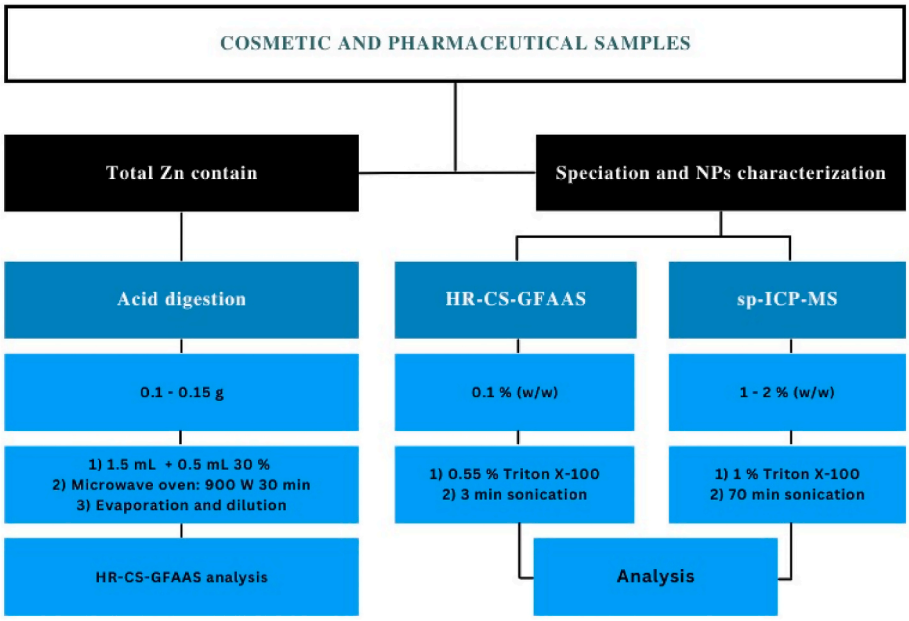

Fig. 1. Scheme of the analytical procedures carried out for the cosmetics samples.

2.4.3. sp-ICP-MS measurement protocol

For the analysis of the different samples, stable suspensions of standards and samples were prepared using Triton X-100 as surfactant. These suspensions were sonicated until homogenization, and then properly diluted. The transport efficiency (TE) is one of the most important sp-ICP-MS parameters. TE is defined as the ratio between the number of particles or mass flux of sample solution entering in the plasma and the particles or mass flux of sample solution introduced in the instrument nebulizer. This parameter is used to transform the signal peak net intensity of a NP into size information with a curve calibration of the mass flux. In this case, the size calibration method described by Pace et al., was used [35]. In this method, TE is calculated as a ratio between the solved metal concentration and nanoparticular calibration slopes. Solved metal (performed using 1–4 μg L^{-1} Au standard solutions) and nanoparticular (performed with the PerkinElmer 100 nm Au NPs standard solution) calibrations were daily prepared. The NP calibration was carried out using just one standard solution (one point calibration) as described by Aramendía et al. [36]. All the standards were diluted with ultrapure water in order to obtain a particle number concentration of at least 1000 NPs mL^{-1}, to avoid the appearance of multiple events. Then, TE was calculated as the ratio of both calibrations, this parameter was always found in the 4–6 % range. For the ZnO NPs analysis in the samples, an ionic Zn calibration was performed using standards with concentrations between 10 and 50 μg L^{-1}, relating the NP signal intensity with the mass concentration (μg).

2.5. Data processing

The obtained results in all the performed analysis were needed of additional data treatments. Two different analyses were done: a) speciation and determination of Zn species, and b) ZnO NPs size characterization. A data treatment protocol was applied depending on the analysis. All the samples were equally processed, taking the same criteria in all cases.

2.5.1. HR–CS–GFAAS data treatment

The spectra data obtained with the software ASPECT CS were exported to comma-separated values (CSV) file format. Then, with the aid of a web service programmed in JavaScript, the pixel 101 was selected to represent the spectrum. Following the previous work [25], the data were treated with the same protocol for the deconvolution of the signals. In this work, the solid suspension methodology showed an advantage in comparison with the direct solid sampling analysis on GFAAS due to the signals of the species are separated from each other, thus the deconvolution was easier. The integrated area for each peak was used for speciation of Zn^{2+}/ZnO NPs in the standards (mixture both species) and samples. In the case of total zinc in the samples, the integrated area for the only peak obtained after digestion of the samples was used.

For the size characterization, experiments were performed to determine the ZnO NPs size through the second atomization peak. For this, calibration curves were obtained with suspensions of solid standards of these NPs of different sizes in 0.55 % Triton X-100. This calibration is showed in SM1. One atomization peak at 5.8 s was observed when ZnO NPs standards were measured, according to the chemical composition of the suspension (only nanoparticular). In the samples, two atomization peaks were found according to the presence of both species. The measure of the upslope of the second peak of the atomization signals (atomization rate, k_{at}) was used for the calibration purposes. The nanoparticular signals were deconvoluted to avoid the small contribution of ionic Zn near to the ZnO NPs region. The results obtained were validated by TEM and compared with the obtained ones by sp-ICP-MS.

2.5.2. sp-ICP-MS data treatment

According to the previous work [36], an in-house developed script written in GNU Octave was used to process the raw data provided by the software. The output signal consists of one-time column with a data value every 100 μs (or the dwell time selected for the analysis performed) and another one containing the net intensities for every NP detected. The script integrates the NP total signal summatory and differentiate them from the background signal. Size calculations, concentrations and graphical representations were carried out using Microsoft Excel (Redmond, Washington, USA) and OriginPro (OriginLab, Northampton, MA, USA).

Several parameters were used to calculate the ZnO NPs size in the samples. First, the ICP-MS response in counts/μg L^{-1} was determined using the slope value of a calibration curve of ionic Zn (10–50 μg L^{-1}) plus the calculation of the TE. According to this method, the TE was calculated following *equation (1)*, where S_{ion} is the slope of the

calibration curve with ionic Au standards (counts/μg L^{-1}; for calculation of this slope, 1–4 μg L^{-1} of Au were considered), S_{NP} is the slope of the calibration curve with the PerkinElmer 100 nm Au NPs (counts/μg L^{-1}; for calculation of this slope, a diluted standard of 100 nm Au NPs was considered), Q_1 is the sample flow rate introduced in the ICP-MS instrument t_{dwell} is the dwell time (s) and 60 is the conversion factor from minutes to seconds. Additionally, the mass (fg) for each NP detected with this method ($m_{NP,IC}$) can be calculated via *equation (2)* taking into account that Zn mass was measured first, and then a mass fraction of 80 % was used to convert the Zn mass to ZnO mass since the ratio of Zn/ZnO is 80 % by weight.

Spherical shapes were assumed to convert the mass of ZnO into diameter information, as these nanoparticles have geometrical irregular shapes. Then, the diameter (nm) of each unknown particle detected (d_{NP}) was subsequently calculated according to *equation (3)*, where m_{NP} refers to the mass of each detected NP calculated according to *equation (2)* (fg), while ρ is the known density of the targeted particle (g cm^{-3}). For this parameter, values included in Table 1 were used for the different NPs analysed.

$$TE = \frac{\frac{S_{ion}}{Q_1 \bullet \left(t_{dwell}/60\right)}}{S_{NP}} \cdot 10^{-3} \quad (1)$$

$$m_{NP,IC} = \frac{I_{NP} \bullet \frac{t_{dwell} \bullet Q_1}{60} \bullet TE}{S_{ion}} \quad (2)$$

$$d_{NP} = \sqrt[3]{\frac{6 \bullet m_{NP}}{\pi \bullet \rho}} \bullet 10^2 \quad (3)$$

OriginPro software was used to extract the data for calculations and graphical representations. Mathematical Gaussian fittings were performed for all the histograms, being the average predicted value (in counts) predicted by the program (X_c) used in the calibration curves.

2.6. Optimization strategy

Preliminary tests were performed with suspensions in two different surfactants (SDS and Triton X-100). Else, in the case of GFAAS, dilutions 1:10, 1:100, and 1:1000 in deionized water were studied, and for sp-ICP-MS higher magnitude orders (10^4, 10^5, 10^6) were tested according to the single particle theory. The instrumental parameters used for GFAAS and for sp-ICP-MS were the presented in Tables 1 and 2, respectively. For these studies, 50 nm ZnO NPs, cream A, and cream B were used.

Multiple response designs were carried out to optimize the slurry preparation. First, considering the surfactant concentrations and sonication times used in the preliminary tests, the lower and upper values of the design variables were stablished between 0.1 and 1 % and 10–60 min respectively. Three response functions were chosen to optimize the slurry preparation for GFAAS: ionic peak height, nanoparticular peak height, and distance between peaks (Spectr. No), and two response function for sp-ICP-MS: the number of particles detected and the background signal (ionic Zn). In all cases, the response functions were maximized except the background signal for sp-ICP-MS, which was minimized. Every experiment was performed in triplicate.

A central composite design plus star was the response surface design chosen for optimize the slurry preparation for each technique where $2^k + 2\ x\ k + n$ runs were generated, being k the number of parameters to optimize ($k = 2$). Attending to this, 2^2 are the points from the factorial experiments carried out at the corners of the cube and $2\ x\ 2$ are the points carried out on the face centred star. The repetition of the central point was used to estimate the experimental error ($n = 2$) in the design. The resulting 10 experiments of the design were randomly performed in both techniques. Statgraphics Centurion software (version 16.1.11 for Windows) was used for processing the experimental data. Analysis of the variance (ANOVA) and p-value significance levels were used for checking the significance of the effects in the design. After this optimization, some variables were studied out of the initial considered range to observe and improve the behaviour of the signal.

All the samples were analysed by TEM, in two different media to compare and validate the results obtained, and for studying the possible particles agglomerations caused by the different surfactants.

3. Results and discussion

The research group, previously, had optimized the speciation of Zn^{2+} and ZnO NPs in different eyeshadows by HR–CS–GFAAS [25]. In the case of the ZnO NPs, the size information was not studied due to the non-reproducibility of the results obtained. This can be explained attending to the different sizes of the ZnO NPs contained in the eyeshadow samples. Moreover, the analysis of pharmaceutical products with more complex matrices such as creams was not possible as this kind of samples present multitude of excipients and high fat contains. In this work, the main purpose was the development of Zn speciation method and size characterization of ZnO NPs, suitable for the analysis in creams, lotions, and eyeshadows. For this purpose, two different instrumental techniques were used: HR–CS–GFAAS and sp-ICP-MS. Therefore, this work can be considered as a more advanced analytical method which provides size and content information for Zn speciation in cosmetics and pharmaceutical samples.

As reported in literature [21,37], the use of surfactants to obtain stable suspensions of NPs is widely extended for sp-ICP-MS analysis as it facilitates the sample introduction. On the other hand, pharmaceutical samples as creams and lotions were not possible to study on the previous work [25] because of the complex matrices, and the signals saturation. So, the first test carried out in this work was the analysis of the selected samples using different surfactants to introduce them as a slurry in the GFAAS and ICP-MS. These preliminary tests were described in section 2.6. Optimization strategy.

In the case of sp-ICP-MS analysis, some observations should be considered. The pulses of NPs are known to have durations between 300 and 500 μs. Considering that dwell times applied are in the range of 100 μs, the NPs pulses are going to be composed of several events. Therefore, the raw data of the sp-ICP-MS analysis need to be processed to recognize these signals, and the background needs to be rested to obtain a good NP information. In the case of ZnO NPs, the analysis by this technique presents several drawbacks: 1) high contamination which means a high ionic baseline, 2) the particles are not composed by only one element, and 3) Zn presents four isotopes so the signal for each NP pulse will be reduced. Moreover, complex matrices, such as the samples studied in this work, make analysis even more difficult. To solve these problems, once the analysis methodology and sample preparation were optimized, the data treatment of the raw data included the calculation of an integration threshold (5s-criterion, 5 times the standard deviation of the background) to filter the ionic contribution as much as possible.

3.1. Preliminary tests

As described in section 2.6, preliminary tests were performed to study the signals obtained of Zn^{2+} and ZnO NPs by both techniques. In Fig. 2 can be seen both signals obtained. In GFAAS analysis (Fig. 2A), two peaks separated in time were obtained with Triton X-100, the first one was identified as the ionic signal (Zn^{2+}) and the second one (with a shoulder), more delayed, corresponding to the ZnO NPs. For sp-ICP-MS, a constant background signal was obtained due to the ionic Zn, and different pulses appeared due to the presence of ZnO NPs in the sample (Fig. 2B). The results of the preliminary tests can be divided into two groups: 1) Selection of the surfactant, and 2) Selection of the slurry concentration in the surfactant. The best conditions were selected based on these results and then a more detailed optimization was performed.

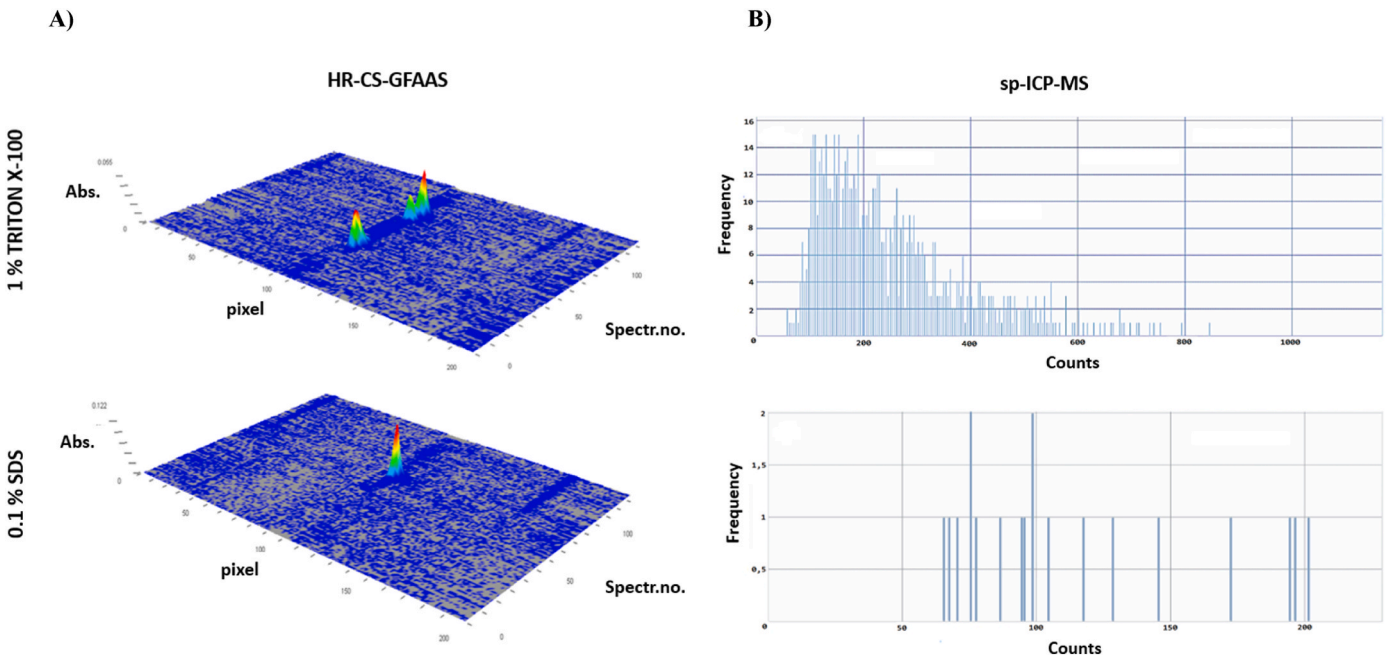

Fig. 2. Signals obtained by both analysis techniques when different surfactants are used for sample preparation. A) For HR–CS–GFAAS analysis; B) For sp-ICP-MS analysis.

3.1.1. *Surfactant selection*

For this analysis, suspensions of ZnO NPs in 1 % Triton X-100 and 0.1 % SDS were prepared and tested. Cream A and 50 nm ZnO NPs standard were used for GFAAS and sp-ICP-MS, respectively. In both cases the sample was prepared as 0.1 % (w/w) and sonicated for 1 h. In the case of sp-ICP-MS, the 50 nm ZnO NPs were properly diluted to detect at least 1000 particles. As can be observed in Fig.2, 1 % Triton X-100 reported better results than 0.1 % SDS, appearing only one peak in the 3-Dimensional (3D) GFAAS spectrum, and less intense signals via sp-ICP-MS. Since both techniques reported more favourable results with Triton X-100, this surfactant was selected for the rest of the studies.

3.1.2. *Slurry concentration study*

Considering that cosmetic and pharmaceutical samples have complex matrices and high Zn concentrations (% levels), a study of the appropriate dilution for analysis was carried out. ICP-MS and GFAAS are very sensitive techniques that can detect levels below μg L^{-1}, so the range of concentrations analysed must be adjusted.

In the case of GFAAS, a secondary wavelength of Zn (307.590 nm) was used [25] to avoid the signal saturation. In this case, measurements of the slurry (0.1 % w/w in 1 % Triton X-100), and 1:10, 1:100 and 1:1000 dilutions of the slurry in deionized water were carried out, and different volumes of these samples were pipetted onto the graphite furnace platform (5, 10, 15 and 20 μL). In this way, the amount of sample analysed was studied. At higher slurry dilutions only one atomization peak was observed at 5.5 s, but when the amount of sample on the platform was increased, an additional atomization peak was observed at 2 s (slurry, and its 1:10 and 1:100 dilutions). To identify the atomization peaks, another test was carried out using Cream A (20 % w/w ZnO according to manufacturer), a 30 mg L^{-1} Zn^{2+} standard and a 50 nm ZnO NPs standard suspension. The Zn^{2+} and ZnO NPs standard solutions were prepared at 0.1 % suspended in 1 % Triton X-100 and analysed separately. In Fig. 3 is shown as the first peak belonged to the ionic contribution of the sample, and the second one to the nanoparticular (larger). The shoulder of the second peak poses contributions of both species. The separation of the atomization peaks is achieved thanks to the surfactant. The reason could be that Triton X-100 favours the agglomeration of the particles delaying their atomization, while the

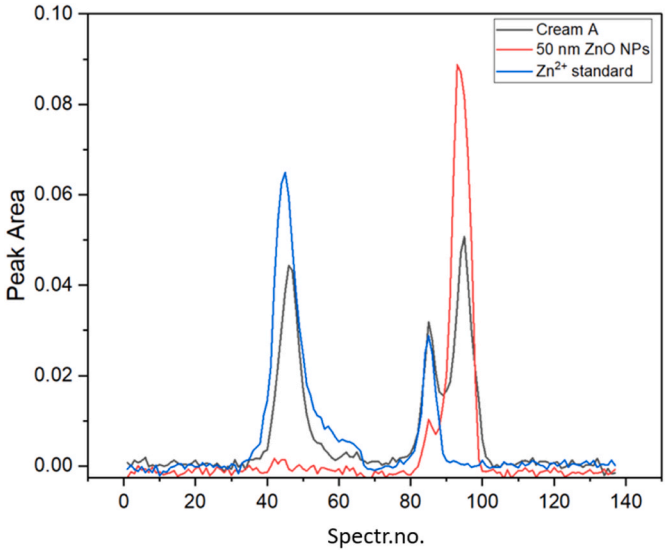

Fig. 3. Identification of the atomization peaks for Zn^{2+} and ZnO NPs in Cream A.

Zn^{2+}, in smaller proportion, is released and atomized earlier. As conclusion, slurry (0.1 % w/w in 1 % Triton X-100) dilutions not higher than 1:1000 are finally selected.

However, in sp-ICP-MS higher slurry dilutions were needed to decrease the background signal (ionic contribution) and to avoid double events, keeping at the same time an adequate number of detected particles, which represent the size distribution. Furthermore, considering the high sensitivity of ICP-MS, as well as, the complexity of the sample matrices studied, commercial ZnO NPs standards were used to carry out preliminary studies and the optimization strategy. A slurry of the 50 nm ZnO NPs (49.99 % ZnO) was prepared as the content of this standard is very similar to many commercial creams used for baby skincare. For this, 0.1 % of the standard was first suspended in 1 % Triton X-100, and then 10^4, 10^5 and 10^6 dilutions were prepared with deionized water.

Once measured, it was observed that 10^6 was enough to detect at least 1000 NPs, generating an intense enough histogram to represent the size distribution of the sample. In this kind of commercial samples, the NPs are not monodispersed, and different sizes of the ZnO NPs are present at different dilutions. For this reason, a wide range of sizes were obtained, and the size distribution histogram did not present a gaussian fitting.

3.2. Optimization results

In order to improve the signals obtained several experimental parameters were subjected to optimization process. To carry out the optimization, Cream A (20 % w/w ZnO according to manufacturer) and 50 nm solid standard ZnO NPs (49.99 % w/w) were used for GFAAS and sp-ICP-MS, respectively.

First, the effect of surfactant concentration and sonication time were studied. Sample suspensions were prepared in Triton X-100. In all cases the sample concentration was 0.1 % (w/w). According to section 2.6., two multiple response designs were carried out, one for each technique. Three-dimensional representations of the response surfaces, being the conditions with the higher desirability the optimal conditions, are shown in Fig. 4A and B. The data indicate that interactions usually occur between principal factors. This means that the response surfaces in the factorial space are curved in the domain of the experimental design. Based on these results, the optimal conditions were: 0.55 % Triton X-100 and 3 min sonication time for GFAAS, and 1 % Triton X-100 and 70 min sonication time for sp-ICP-MS.

Additional experiments were performed according to the conclusions obtained from the response surfaces. For the sonication time, the optimum value was the lowest in the design, for GFAAS, and the highest in the response surface for sp-ICP-MS, so lower and higher values than 3 and 70 min respectively were tested in each case.

Based on the results of these assays, the conclusions were that sonication time had no influence on the signals of the samples by GFAAS, and in contrast for sp-ICP-MS the best results were obtained at 90 min. In single particle, a great homogenization of the suspension is important since short fast measurements are performed at a constant flow rate. This high sonication time was also studied to evaluate if this factor provides the dissolution of the NPs, increasing the ionic background, and no drawbacks were found.

With the slurry conditions optimized, the instrumental conditions for HR–CS–GFAAS (pyrolysis, atomization temperature, and use of chemical modifiers) were studied starting from those established in our previous work [25]. The results of these experiments showed that the initial conditions were the best ones for the speciation analysis, Table 1.

As an example, the signals obtained with the optimized experimental parameters for Cream C using the two studied techniques, are shown in Fig. 5A and B. Also, the TEM image for the same sample, suspended in ethanol, is shown in Fig. 5C. The 3D spectrum by GFAAS (Fig. 5B) was in concordance with the composition of the samples since in the baby creams (A, B and C), the ZnO NPs contents are around 20–40 % (w/w), and the amount of ionic Zn is quite less.

3.3. Analytical applications

Once the optimal conditions were established, the analysis of the selected samples was carried out. In order to validate the results obtained, other protocols and techniques were applied. For the validation of the concentrations of both Zn species, total Zn content was determined in digested samples, and TEM was used for the validation of ZnO NPs size determination.

3.3.1. Zn^{2+}/ZnO NPs speciation

The GFAAS analysis was applied to the study of three baby skin care creams (creams A, B, and C) and two lotions (lotions 1 and 2), all of them with high Zn content. The results obtained from the speciation analysis of Zn^{2+} and ZnO NPs, both expressed as percentage of Zn, were well-compared with the total Zn content obtained in the analysis of the digested samples, and with the total Zn content specified by the pharmaceutical company (creams A and C). One eyeshadow studied under solid sampling analysis in our previous work [25] was also analysed using the slurry methodology proposed in this work. The results obtained for both methodologies (solid sampling and slurry formation) were in good concordance, validating the method also for eyeshadows. These results are shown in Table 3. In the case of the creams, the total Zn contents (specified by the pharmaceutical company) expressed in percentage of Zn^{2+}, were 16 and 32 %, for creams A and C, respectively, being ZnO NPs the main species of Zn contained in the sample due to its antiseptic function by acting as a barrier against external agents. Between the three cream samples analysed, from a qualitative point of view, Creams A and C were pastier and more whitish, according with the approximate NP content indicated by the manufacturer. However, Cream B (which does not indicate content) presented a much more fluid texture, confirming the amount of ZnO NPs determined, which was much lower than Creams A and C. In the case of the lotions, the appearances were less whitish and more liquid, which corresponds to their lower NP content. In all cases, the sum of ZnO NPs and Zn^{+2} concentration agrees with the total Zn content determined.

To validate these results, a statistical analysis was carried out with Student's *t*-test for paired samples between the sum of the speciation analysis (expressed in Zn^{2+}) and the results obtained by total digestion analysis. No significant differences ($t_{exp} = 1.08 < t_{tab} = 2.26$) were found. Other *t*-test for paired samples between the total acid digestion results and specified data by the manufacturers (creams A and C) and the eyeshadow 4 (Gloss grey eyeshadow, previously analysed in our previous work) was performed and no significant differences ($t_{exp} = 1.34 < t_{tab} = 4.30$) were also found. In conclusion, GFAAS technique is a good analytical tool to perform speciation analysis of complex samples without needing complex sample treatments.

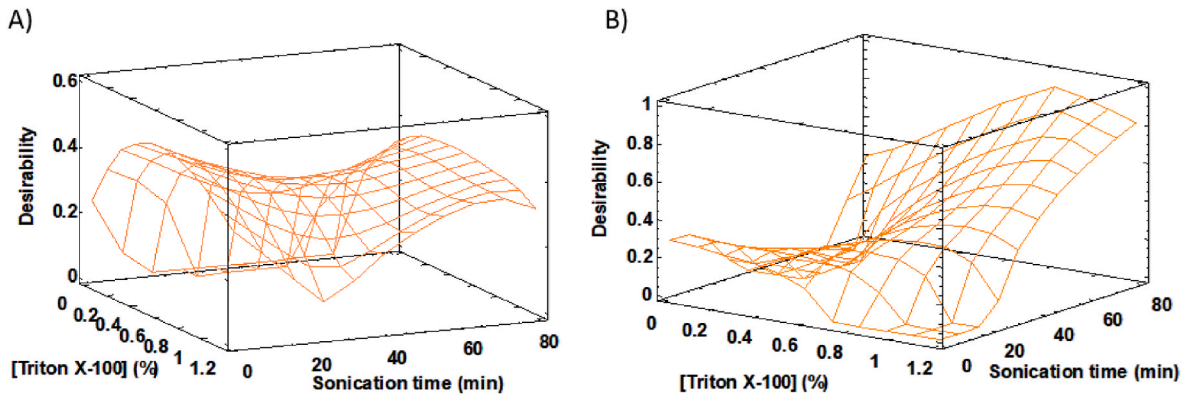

Fig. 4. Response surface obtained for the simultaneous optimization of Triton X-100 concentration and the sonication time in: A) HR–CS–GFAAS and B) sp-ICP-MS.

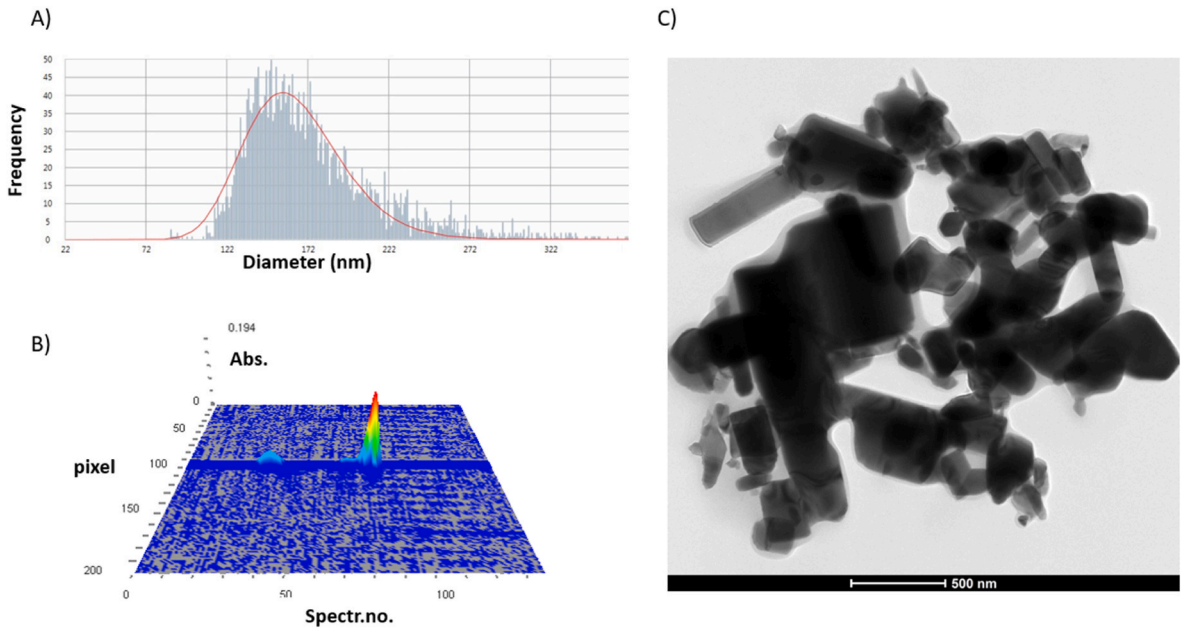

Fig. 5. Cream C under optimal conditions in **A)** sp-ICP-MS; **B)** HR–CS–GFAAS; and **C)** TEM.

Table 3
Zn speciation analysis of pharmaceutical and cosmetic samples.

Zn content (%)				
Sample	HR–CS–GFAAS			Total acid digestion
	Zn^{2+}	*ZnO NPs*	***Total***	
Eyeshadow 4	0.04 ± 0.01	0.28 ± 0.05	**0.32 ± 0.05**	**0.30 ± 0.09**[a]
Cream A	1.08 ± 0.09	16 ± 1	**17 ± 1**[b]	**16.4 ± 1.0**
Cream B	1.4 ± 0.2	6.5 ± 0.1	**8.0 ± 0.2**	**11 ± 3**
Cream C	1.5 ± 0.3	31.5 ± 0.2	**33.0 ± 0.4**[c]	**34 ± 4**
Lotion 1	1.3 ± 0.3	0.7 ± 0.1	**2.0 ± 0.3**	**2.0 ± 0.5**
Lotion 2	1.2 ± 0.4	0.7 ± 0.3	**1.8 ± 0.5**	**1.9 ± 0.3**

*All data are expressed in Zn^{2+}% applying the ratio between molecular weights (Zn/ZnO) to convert the ZnO %.

[a] Total Zn content (%): 0.33 ± 0.02 (% Zn^{2+} + ZnO NPs) and 0.30 ± 0.02 (SS-HR–CS–GFAAS) [25].

[b] 16 % specified by the pharmaceutical company.

[c] 32 % specified by the pharmaceutical company.

Table 4
ZnO NPs size analysis of pharmaceutical and cosmetic samples.

ZnO NPs size (nm)				
Sample	HR–CS–GFAAS	sp-ICP-MS	TEM (ethanol)	TEM (1 %Triton X-100)
Eyeshadow 1	130 ± 27	100 ± 16	92 ± 20	117 ± 26
Eyeshadow 2	103 ± 58	104 ± 24	100 ± 24	117 ± 28
Eyeshadow 3	87 ± 16	73 ± 5	103 ± 25	116 ± 11
Eyeshadow 4	109 ± 3	79 ± 2	93 ± 15	105 ± 16
Eyeshadow 5	135 ± 35	72 ± 6	77 ± 17	78 ± 10
Cream A	137 ± 15	129 ± 5	132 ± 28	134 ± 29
Cream B	143 ± 14	138 ± 24	148 ± 28	144 ± 24
Cream C	230 ± 51	157 ± 3	198 ± 51	232 ± 62
Lotion 1	–	–	–	–
Lotion 2	–	–	–	–

For the analysis by sp-ICP-MS, the speciation analysis was not possible, attending to the drawbacks that this technique presents for Zn analysis and for complex matrices. Unfortunately, significant dissolution of the NPs generally increases background levels of dissolved ions, making very difficult the speciation. This effect was observed for Ag NPs sp-ICP-MS analysis by Luo et al. [38].

3.3.2. ZnO NPs size determination

The size analysis was carried out through HR–CS–GFAAS, sp-ICP-MS, and TEM. The obtained data were compared and validated with the obtained by TEM analysis in Table 4. In the case of eyeshadows and creams the ZnO NPs size were obtained through the two developed methods. However, the ZnO NPs lotions size could not be provided because of the low content of NPs. This was verified with the TEM analysis, being not found NPs in lotion 1 and lotion 2 and, also in the speciation analysis (3.3.1) the contents found in these samples were mostly Zn^{2+}.

Considering that real samples are commercials, the nanoparticle contents present high dispersions, and the standard deviations of the size data are also high. Taking in account that surfactants can origin agglomerates between the particles, TEM analysis was carried out in two different media: ethanol (used in commercial standards by manufacturers of ZnO NPs), and 1 % Triton X-100 (this work conditions). A Student's t-test for paired samples was performed between the TEMs analysis and $t_{exp} = 2.53 > t_{tab} = 2.26$ showing that the Triton X-100 cause some agglomerates in the particles. This Student's t-test was also carried out between both studied techniques and TEM results, showing that in the case of sp-ICP-MS agglomerates affect more than in the case of GFAAS. Finally, analysis of the variance (ANOVA) and p-value significance levels were checked for validation, and no significant differences were found ($F_{tab} = 2.87 > F_{exp} = 0.26$) For this comparison, a box and whisker plot are presented in Fig. 6.

4. Conclusions

The two innovative techniques used in this work allow the characterization of ZnO NPs size distribution in real samples with complex matrices such as cosmetics, creams, and lotions. The size information of NPs is provided thanks to the correlation between NP size and the upslope of the atomization peak in HR–CS–GFAAS and is also obtained with the calculations of sp-ICP-MS analysis. Moreover, a previous

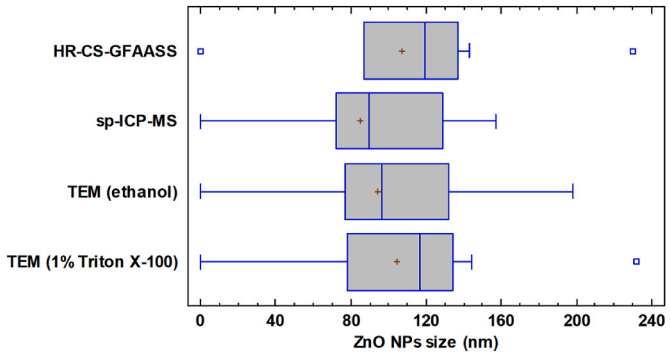

Fig. 6. Box and whisker plot for the different size analysis results comparison.

methodology developed by our research group for solid sampling analysis using HR–CS–GFAAS has been improved with the preparation of slurries. In this way, the speciation of Zn^{2+} and ZnO NPs has been carried out successfully in creams and lotions. The use of surfactant such as Triton X-100 provides advantages: 1) Solid (eyeshadows) and pasty (creams and lotions) samples can be easily introduced in the ICP-MS for the single particle analysis, simply preparing a suspension, 2) The surfactant allows a better separation of the HR–CS–GFAAS atomization peaks facilitating the speciation analysis in all types of cosmetics samples, including creams and lotions, and 3) Data treatments to obtain the size information in GFAAS are simpler and faster with a deconvolution of the second peak. These new methodologies open the possibility of obtaining nanoparticles size information in real samples using instruments currently present in routine laboratories. If both methodologies are compared, the HR–CS–GFAAS method is cheaper, and the data treatments are simpler and faster, also enables speciation. On the other hand, most of the works in the bibliography applying sp-ICP-MS to the analysis of NPs are only model methods with not real samples (just known size and concentration standards or certified standards). Complex matrices are hard to deal with in single particle, so new strategies, as the described in this work, to get information in that kind of samples are necessary.

The results obtained for the 10 studied samples were validated with a conventional TEM technique for size information, and with total digestion analysis on GFAAS for the speciation analysis. For GFAAS both analyses can perform together only introducing a size calibration, and in the case of sp-ICP-MS NPs size distribution can be easily obtained with the optimized method, nevertheless the speciation is difficult according to the complexity of cosmetics and pharmaceutical samples. Authors agrees with the importance of developing this kind of strategies considering how widely used are NPs in everyday life.

Credit author statement

E.I. Vereda Alonso: Conceptualization, Methodology, Formal analysis, Writing – original draft, Writing – review & editing, Software, Data curation, Supervision, Resources, Funding acquisition. M.M. López Guerrero: Conceptualization, Methodology, Formal analysis, Writing – review & editing, Data curation, Supervision, Resources. I. Morales Benítez: Investigation, Methodology, Writing – review & editing, Validation, Software, Formal analysis, Data curation. P. Montoro Leal: Investigation, Methodology, Writing – review & editing, Validation, Software, Formal analysis, Data curation. J.C. García-Mesa: Investigation, Methodology, Writing – review & editing, Validation, Software, Formal analysis, Data curation. All authors have read and agreed to the published version of the manuscript.

Declaration of competing interest

The authors declare that they have no known competing financial interests or personal relationships that could have appeared to influence the work reported in this paper.

Data availability

Data will be made available on request.

Acknowledgements

The authors thank the University of Málaga (Proyecto Puente B4-2023-19 and predoctoral grant A.2.2021), Spanish Ministerio de Ciencia e Innovación (Project PID2021-126794OB-100) for supporting this study, the Spanish Ministerio de Ciencia y Tecnología for the fellowship FPU18/05371 and Junta de Andalucía for Garantía Juvenil program. Funding for open access charge: Universidad de Málaga/CBUA.

Appendix A. Supplementary data

Supplementary data to this article can be found online at https://doi.org/10.1016/j.talanta.2023.125360.

References

[1] M.H. Kathawala, K.W. Ng, S.C.J. Loo, TiO2 nanoparticles alleviate toxicity by reducing free Zn2+ ion in human primary epidermal keratinocytes exposed to ZnO nanoparticles, J. Nanoparticle Res. 17 (2015) 263, https://doi.org/10.1007/s11051-015-3068-4.
[2] R. Aznar, F. Barahona, O. Geiss, J. Ponti, T. José Luis, J. Barrero-Moreno, Quantification and size characterisation of silver nanoparticles in environmental aqueous samples and consumer products by single particle-ICPMS, Talanta 175 (2017) 200–208, https://doi.org/10.1016/j.talanta.2017.07.048.
[3] A.R. Donovan, C.D. Adams, Y. Ma, C. Stephan, T. Eichholz, H. Shi, Single particle ICP-MS characterization of titanium dioxide, silver, and gold nanoparticles during drinking water treatment, Chemosphere 144 (2016) 148–153, https://doi.org/10.1016/j.chemosphere.2015.07.081.
[4] S. Ansar, M. Abudawood, A.S.A. Alaraj, S.S. Hamed, Hesperidin alleviates zinc oxide nanoparticle induced hepatotoxicity and oxidative stress, BMC Pharmacol Toxicol 19 (2018) 65, https://doi.org/10.1186/s40360-018-0256-8.
[5] R. Peters, Z. Herrera-Rivera, A. Undas, M. van der Lee, H. Marvin, H. Bouwmeester, S. Weigel, Single particle ICP-MS combined with a data evaluation tool as a routine technique for the analysis of nanoparticles in complex matrices, J Anal At Spectrom 30 (2015) 1274–1285, https://doi.org/10.1039/C4JA00357H.
[6] P.-J. Lu, S.-C. Huang, Y.-P. Chen, L.-C. Chiueh, D.Y.-C. Shih, Analysis of titanium dioxide and zinc oxide nanoparticles in cosmetics, J. Food Drug Anal. 23 (2015) 587–594, https://doi.org/10.1016/j.jfda.2015.02.009.
[7] A.M. Holmes, Z. Song, H.R. Moghimi, M.S. Roberts, Relative penetration of zinc oxide and zinc ions into human skin after application of different zinc oxide formulations, ACS Nano 10 (2016) 1810–1819, https://doi.org/10.1021/acsnano.5b04148.
[8] P.C. Nagajyothi, S.J. Cha, I.J. Yang, T.V.M. Sreekanth, K.J. Kim, H.M. Shin, Antioxidant and anti-inflammatory activities of zinc oxide nanoparticles synthesized using Polygala tenuifolia root extract, J. Photochem. Photobiol., B 146 (2015) 10–17, https://doi.org/10.1016/j.jphotobiol.2015.02.008.
[9] H. Mirzaei, M. Darroudi, Zinc oxide nanoparticles: biological synthesis and biomedical applications, Ceram. Int. 43 (2017) 907–914, https://doi.org/10.1016/j.ceramint.2016.10.051.
[10] A. Kahru, H.-C. Dubourguier, From ecotoxicology to nanoecotoxicology, Toxicology 269 (2010) 105–119, https://doi.org/10.1016/j.tox.2009.08.016.
[11] V.L. Pachapur, A. Dalila Larios, M. Cledón, S.K. Brar, M. Verma, R.Y. Surampalli, Behavior and characterization of titanium dioxide and silver nanoparticles in soils, Sci. Total Environ. (2016) 933–943, https://doi.org/10.1016/j.scitotenv.2015.11.090, 563–564.
[12] I. de la Calle, M. Menta, F. Séby, Current trends and challenges in sample preparation for metallic nanoparticles analysis in daily products and environmental samples: a review, Spectrochim. Acta Part B At. Spectrosc. 125 (2016) 66–96, https://doi.org/10.1016/j.sab.2016.09.007.
[13] B. Bocca, S. Caimi, O. Senofonte, A. Alimonti, F. Petrucci, ICP-MS based methods to characterize nanoparticles of TiO2 and ZnO in sunscreens with focus on regulatory and safety issues, Sci. Total Environ. 630 (2018) 922–930, https://doi.org/10.1016/j.scitotenv.2018.02.166.
[14] R. Peters, Z. Herrera-Rivera, A. Undas, M. van der Lee, H. Marvin, H. Bouwmeester, S. Weigel, Single particle ICP-MS combined with a data evaluation tool as a routine technique for the analysis of nanoparticles in complex matrices, J Anal At Spectrom 30 (2015) 1274–1285, https://doi.org/10.1039/C4JA00357H.
[15] L. Fréchette-Viens, M. Hadioui, K.J. Wilkinson, Quantification of ZnO nanoparticles and other Zn containing colloids in natural waters using a high sensitivity single particle ICP-MS, Talanta 200 (2019) 156–162, https://doi.org/10.1016/j.talanta.2019.03.041.

[16] A.C. Gimenez-Ingalaturre, K. Ben-Jeddou, J. Perez-Arantegui, M.S. Jimenez, E. Bolea, F. Laborda, How to trust size distributions obtained by single particle inductively coupled plasma mass spectrometry analysis, Anal. Bioanal. Chem. (2022), https://doi.org/10.1007/s00216-022-04215-z.
[17] Y. Dan, W. Zhang, R. Xue, X. Ma, C. Stephan, H. Shi, Characterization of gold nanoparticle uptake by tomato plants using enzymatic extraction followed by single-particle inductively coupled plasma–mass spectrometry analysis, Environ. Sci. Technol. 49 (2015) 3007–3014, https://doi.org/10.1021/es506179e.
[18] I. Strenge, C. Engelhard, Capabilities of fast data acquisition with microsecond time resolution in inductively coupled plasma mass spectrometry and identification of signal artifacts from millisecond dwell times during detection of single gold nanoparticles, J Anal At Spectrom 31 (2016) 135–144, https://doi.org/10.1039/C5JA00177C.
[19] V. Kantorová, M. Loula, A. Kaňa, O. Mestek, Determination of silver nanoparticles in cosmetics using single particle ICP-MS, Chem. Pap. 75 (2021) 5895–5905, https://doi.org/10.1007/s11696-021-01763-z.
[20] J.-L. Wang, E. Alasonati, M. Tharaud, A. Gelabert, P. Fisicaro, M.F. Benedetti, Flow and fate of silver nanoparticles in small French catchments under different land-uses: the first one-year study, Water Res. 176 (2020), 115722, https://doi.org/10.1016/j.watres.2020.115722.
[21] Y. Dan, H. Shi, C. Stephan, X. Liang, Rapid analysis of titanium dioxide nanoparticles in sunscreens using single particle inductively coupled plasma–mass spectrometry, Microchem. J. 122 (2015) 119–126, https://doi.org/10.1016/j.microc.2015.04.018.
[22] S. Salou, C.-M. Cirtiu, D. Larivière, N. Fleury, Assessment of strategies for the formation of stable suspensions of titanium dioxide nanoparticles in aqueous media suitable for the analysis of biological fluids, Anal. Bioanal. Chem. 412 (2020) 1469–1481, https://doi.org/10.1007/s00216-020-02412-2.
[23] O. Geiss, I. Bianchi, C. Senaldi, G. Bucher, E. Verleysen, N. Waegeneers, F. Brassinne, J. Mast, K. Loeschner, J. Vidmar, F. Aureli, F. Cubadda, A. Raggi, F. Iacoponi, R. Peters, A. Undas, A. Müller, A.-K. Meinhardt, E. Walz, V. Gräf, J. Barrero-Moreno, Particle size analysis of pristine food-grade titanium dioxide and E 171 in confectionery products: interlaboratory testing of a single-particle inductively coupled plasma mass spectrometry screening method and confirmation with transmission electron microscopy, Food Control 120 (2021), 107550, https://doi.org/10.1016/j.foodcont.2020.107550.
[24] M. Hadioui, V. Merdzan, K.J. Wilkinson, Detection and characterization of ZnO nanoparticles in surface and waste waters using single particle ICPMS, Environ. Sci. Technol. 49 (2015) 6141–6148, https://doi.org/10.1021/acs.est.5b00681.
[25] J.C. García-Mesa, P. Montoro-Leal, A. Rodríguez-Moreno, M.M. López Guerrero, E. I. Vereda Alonso, Direct solid sampling for speciation of Zn^{2+} and ZnO nanoparticles in cosmetics by graphite furnace atomic absorption spectrometry, Talanta (2020), https://doi.org/10.1016/j.talanta.2020.121795.
[26] F. Gagné, P. Turcotte, C. Gagnon, Screening test of silver nanoparticles in biological samples by graphite furnace-atomic absorption spectrometry, Anal. Bioanal. Chem. 404 (2012) 2067–2072, https://doi.org/10.1007/s00216-012-6258-2.
[27] N.S. Feichtmeier, K. Leopold, Detection of silver nanoparticles in parsley by solid sampling high-resolution–continuum source atomic absorption spectrometry, Anal. Bioanal. Chem. 406 (2014) 3887–3894, https://doi.org/10.1007/s00216-013-7510-0.
[28] N.S. Feichtmeier, N. Ruchter, S. Zimmermann, B. Sures, K. Leopold, A direct solid sampling analysis method for the detection of silver nanoparticles in biological matrices, Anal. Bioanal. Chem. 408 (2016) 295–305, https://doi.org/10.1007/s00216-015-9108-1.
[29] M. Resano, E. Garcia-Ruiz, R. Garde, High-resolution continuum source graphite furnace atomic absorption spectrometry for the monitoring of Au nanoparticles, J Anal At Spectrom 31 (2016) 2233–2241, https://doi.org/10.1039/C6JA00280C.
[30] E. Vereda Alonso, M.M. López Guerrero, M.T. Siles Cordero, J.M. Cano Pavón, A. García De Torres, Characterization of solid magnetic nanoparticles by means of solid sampling high resolution continuum source electrothermal atomic absorption spectrometry, J Anal At Spectrom 31 (2016), https://doi.org/10.1039/c6ja00225k.
[31] A. Brandt, K. Kees, K. Leopold, Characterization of various metal nanoparticles by graphite furnace atomic absorption spectrometry: possibilities and limitations with regard to size and shape, J Anal At Spectrom 35 (2020) 2536–2544, https://doi.org/10.1039/D0JA00279H.
[32] J. Friedland, A. Brandt, K. Leopold, R. Güttel, Atomization of gold nanoparticles in graphite furnace AAS: modelling and simulative exploration of experimental results, Spectrochim. Acta Part B At. Spectrosc. 182 (2021), 106249, https://doi.org/10.1016/j.sab.2021.106249.
[33] J. Gruszka, A. Martyna, B. Godlewska-Żyłkiewicz, Chemometric approach to discrimination and determination of binary mixtures of silver ions and nanoparticles in consumer products by graphite furnace atomic absorption spectrometry, Talanta 230 (2021), 122319, https://doi.org/10.1016/j.talanta.2021.122319.
[34] J.W. Olesik, P.J. Gray, Considerations for measurement of individual nanoparticles or microparticles by ICP-MS: determination of the number of particles and the analyte mass in each particle, J Anal At Spectrom 27 (2012) 1143–1155, https://doi.org/10.1039/c2ja30073g.
[35] H.E. Pace, N.J. Rogers, C. Jarolimek, V.A. Coleman, C.P. Higgins, J.F. Ranville, Determining transport efficiency for the purpose of counting and sizing nanoparticles via single particle inductively coupled plasma mass spectrometry, Anal. Chem. 83 (2011), https://doi.org/10.1021/ac201952t.
[36] M. Aramendía, J.C. García-Mesa, E.V. Alonso, R. Garde, A. Bazo, J. Resano, M. Resano, A novel approach for adapting the standard addition method to single particle-ICP-MS for the accurate determination of NP size and number concentration in complex matrices, Anal. Chim. Acta 1205 (2022), https://doi.org/10.1016/j.aca.2022.339738.
[37] I. de la Calle, M. Menta, M. Klein, F. Séby, Screening of TiO2 and Au nanoparticles in cosmetics and determination of elemental impurities by multiple techniques (DLS, SP-ICP-MS, ICP-MS and ICP-OES), Talanta 171 (2017) 291–306, https://doi.org/10.1016/j.talanta.2017.05.002.
[38] L. Luo, Y. Yang, H. Li, R. Ding, Q. Wang, Z. Yang, Size characterization of silver nanoparticles after separation from silver ions in environmental water using magnetic reduced graphene oxide, Sci. Total Environ. 612 (2018) 1215–1222, https://doi.org/10.1016/j.scitotenv.2017.09.024.